The Action of Interhelical Forces on the Organization of DNA Double Helices: Fluctuation-Enhanced Decay of Electrostatic Double-Layer and Hydration Forces

Rudi Podgornik,† Donald C. Rau, and V. Adrian Parsegian*

National Institutes of Health, Bethesda, Maryland 20892. *Received June 14, 1988; Revised Manuscript Received September 14, 1988*

ABSTRACT: Using the osmotic stress method, we have simultaneously measured the mean repulsive force and the lateral fluctuations in polymer-condensed arrays of parallel DNA double helices in univalent salt solutions. The observed forces do not coincide with the salt-screened electrostatic double-layer forces traditionally expected in this polyelectrolyte system. At molecular surface separations ≤ 10 Å, repulsion varies exponentially with characteristic decay constants, ≃3–3.4 Å, insensitive to ionic species and to ionic strength. (We have previously associated this interaction with the "hydration force" seen earlier between lipid bilayers.) At larger distances, the force is again exponential, though sensitive to salt species and concentration; its decay length, however, is about twice the expected theoretical Debye length, except at very high ionic strengths where it is about twice the 3.4-Å hydration decay length. The continuous increase in lateral fluctuations observed at these larger separations suggests that extended molecular repulsion is due to a progressive increase in configurational entropy, itself due to the onset of positional disorder in the DNA double helices.

Introduction

Recent direct measurements of forces between parallel DNA double helices have made us aware of two unexpected facts: Near contact, intersurface separation ≤ 10 Å, these polyelectrolyte molecules repel with an exponentially decaying force whose ≅3-Å decay constant is virtually independent of ionic strength.[1] We find now that at greater distances salt concentration dependent forces act between the molecules but they are qualitatively modified by configurational fluctuations which are suppressed by soft collisions effected by long-range potentials. At no point does the force vary in the way expected from traditional double-layer theory.

Indeed, this behavior is not completely unexpected. For over a decade, osmotic stress measurements of forces between lipid bilayers showed the dominance of powerful hydration forces acting at less than 20–30-Å separation.[2-4] The exponential behavior found there seemed to vary little with the presence of added salt or with the state of charge of the lipid. Charge and ionic strength did affect the point of transition, at 15–25-Å separation, to a region of electrostatic double-layer interaction. The puzzle was that even here these forces decayed more slowly than expected from Debye–Hückel screening length,[4-6] while electrostatic forces between comparatively rigid surfaces seemed to display the traditional screening length.[7,8]

One solution to this puzzle was proposed by Evans and Parsegian,[9] extending the ideas of Helfrich,[10] who suggested that as bilayers were allowed to move apart they became better able to undulate. This progressive onset of undulation constituted an ever increasing contribution of the configurational confinement entropy to the interaction free energy, mediated by the underlying "elastic" force through which neighboring bilayers would "collide".

This interplay between elastic forces and configurational confinement is apparent in the interaction between parallel DNA polymers. In fact, one sometimes sees rather clean regions of purely "elastic", "bare" forces at close separation and of configurational entropy dominated behavior at the larger separations examined in this paper. At these larger separations there is still an exponentially decaying force, but its decay rate is either twice the Debye decay length expected from electrostatic double-layer theory or (in solutions of very high salt concentrations) twice the decay length of the hydration forces measured at small separations.

At the same time that we have determined interhelical forces and distances, we have measured the degree of positional disorder of the DNA chains. (To do so we monitor the progressive sharpening of the X-ray diffraction peaks used to measure molecular separation.) Indeed, it is from this information that we are able to conclude that the observed extraexpansive forces represent the work of removal of configurational degrees of freedom as helices are brought together. Entropic enhancement of the underlying "bare" electrostatic or hydration interactions seems to be an essential feature of assembly in this system.

Materials and Methods

Forces were measured by the osmotic stress technique.[4,11] Double-helical B-DNA in solution, if exposed to a high molecular weight polymer (e.g., poly(ethylene glycol), PEG), condenses into a polymer-free lattice whose well-defined interaxial spacing can be determined from the equatorial X-ray diffraction pattern.[1,12] The osmotic stress acting on the DNA lattice is equal to the osmotic pressure of the polymer solution. One is thus able to determine the force vs separation of parallel DNA double helices in the same way as has been described previously.[1]

We have used high molecular weight (≅10×10^6) native calf thymus DNA (Worthington), dissolved in 0.5 M NaCl (pH ≅7) in 10 mM Tris/1 mM Na EDTA (10/1 TE) buffer ($A_{260} \cong 20$), phenol/chloroform extracted to remove extraneous protein, and exhaustively dialyzed against 10/1 TE buffer to obtain gels for X-ray scattering measurements. The alternating polynucleotides poly(dA-dT) ($M_r \cong 2 \times 10^5$) (Pharmacia) and poly(dG-dC) ($M_r \cong 3 \times 10^6$) (Pharmacia) were phenol/chloroform extracted once and dialyzed directly against 10/1 TE buffer.

Nucleosomal DNA was isolated from fresh chicken blood (≅100 mL) by using the procedure described by Shindo et al.[13] A 6% polyacrylamide gel of the histone-free DNA was used to estimate the DNA size in the core particle to be 145 ± 20 base pairs.

The DNA gels for X-ray diffraction measurements were prepared either by precipitating with 5% poly(ethylene glycol) (PEG 20; MW ≅ 20 000; Sigma) or with ethanol. Thermodynamic equilibrium was verified by occasionally creating pellets by condensing DNA from dilute solution and finding the same properties as those made by expansion of DNA from alcohol precipitates. In both cases, the pellets were centrifuged down and supernatant was replaced with a lower molecular weight poly(ethylene glycol) (PEG 8; MW ≅ 8000; Sigma) solution having a determined osmotic pressure and ionic concentration, in vast excess. The Debye (screening) length of the salt solution was determined from the

* Author to whom correspondence should be addressed.
† On leave from Jožef Stefan Institute, p.p. 100, 61111 Ljubljana, Yugoslavia.

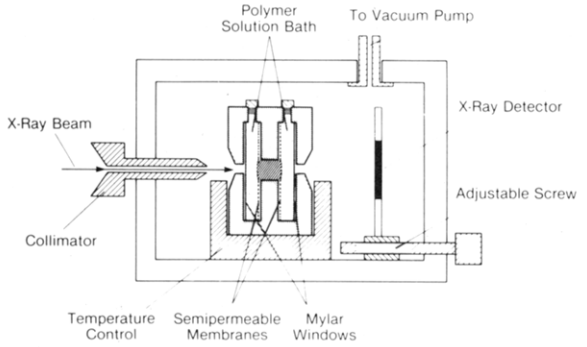

Figure 1. Scheme of osmotic stress method. The sample is separated from the stressing (PEG) solution by a semipermeable membrane while held in the path of an X-ray beam. The PEG solution acts as a spring to measure (or to set) the mean force between DNA molecules; the X-ray diffraction pattern gives the lattice symmetry, the mean molecular separation, and positional disorder.

relation $\lambda_{Debye} \cong 3\ \text{Å}/I^{1/2}$ where I is the molar ionic strength. Osmotic pressures of the PEG 8 solutions were measured by equilibration against PEG 20 solutions, whose pressures were in turn obtained by direct membrane osmometry as described by Leneveu et al.[2] The osmotic pressure of PEG 8 as a function of weight fraction in water can be described accurately by an expression derived by Michel and associates.[14,15] Details about these properties and the osmotic stress method are given in ref 11.

X-ray diffraction pictures were taken at a constant temperature of $T = 20$ °C either with an Elliot GX-20 rotating anode generator or a Phillips fixed anode generator with the Kα Cu emission line of wavelength $\lambda = 1.54$ Å in a setup as shown in Figure 1. Except for the required exposure time, no difference was detected between the quality of the diffraction data from the two setups. The sample to film distance was calibrated from a strong 14.5-Å bromobenzoic acid crystal reflection. The inherent line width of the setup was estimated from the same diffraction pattern and was found to make a negligible contribution to the overall broadening of the diffraction pattern. The interaxial reflection was identified as the most intense ring on the film. Beyond 30 Å, the diffraction rings become increasingly diffuse and the higher order reflections, consistent with the continued hexagonal symmetry, progressively merge with the background. The fine analysis of the diffraction pattern needed to extract a quantitative estimate of the broadness of the first diffraction peak was undertaken after the original diffraction data from the film were digitized through the use of a Perkin-Elmer 1010G microdensitometer and circularly averaged.

To ensure that no major packing change took place in the system at interaxial spacings of 30–50 Å, we have independently observed the texture of the collapsed DNA phase under crossed polarizers. There was no sudden change of the texture, the striations consistent with previous observations[16] gradually becoming wider as the osmotic pressure diminished. At small enough osmotic pressures, where the X-ray reflections were lost, we also failed to observe any texture under the crossed polarizers, a finding indicating that the collapsed DNA had reentered the dispersed phase. In calculations of the interhelical spacings (d_i) we have therefore assumed hexagonal symmetry ($d_i = (2/3^{1/2})d_{Bragg}$) over the whole range of osmotic pressures where a clear Bragg reflection was detectable. Due to the broadening of the diffraction ring, the overall error in the determination of the larger spacings can be as much as ±1.0 Å but is usually less. Probably because of multiple scattering and/or absorption of X-rays by the heavy Cs^+ ions, the Cs-DNA diffraction patterns were weak and did not provide the same accuracy in the spacing determination obtained from other samples. At high Cs^+ concentrations the diffraction pattern was lost altogether.

Broadening of the diffraction pattern, first observed by Maniatis et al.,[12] is due to the onset of positional disorder in the system. To connect the extent of broadening in the wavevector (Q) space with the positional disorder in real space, a microscopic structural theory is needed. ($Q = (4\pi/\lambda) \sin(\vartheta/2)$, where ϑ is the scattering angle; $\vartheta = \arctan(R/L)$ with R the off-center distance and L the detector to sample separation.) There exists none for the collapsed DNA phase. We have therefore used an operational definition of the positional disorder of the DNA chains by applying the theory of molecular disorder of the second kind, as described by Guinier.[17]

The broadening of the diffraction peaks reflects the positional disorder of the Bragg planes. Since the direction of the reflecting planes is arbitrary, the positional disorder of the Bragg planes can in turn be translated into the positional disorder of the interhelical spacings. Following this type of reasoning, we first apply the Gaussian (Guinier) approximation to the probability (H_1) that the first-neighbor Bragg plane is at a distance x that deviates from the mean Bragg spacing d_{Bragg} by an amount u, $u = d_{Bragg} - x$

$$H_1(u) = \frac{1}{((2\pi)\Delta_{Bragg})^{1/2}} \exp(-u^2/2\Delta_{Bragg}^2) \tag{1a}$$

The mean separation is

$$\int_{-\infty}^{+\infty} xH_1(d_{Bragg} - x)\, dx = d_{Bragg} \tag{1b}$$

while the mean square separation is of the form

$$\int_{-\infty}^{+\infty} x^2H_1(d_{Bragg} - x)\, dx = d_{Bragg}^2 + \Delta_{Bragg}^2 \tag{1c}$$

Guinier has shown (eq 9.5 of ref 17) that the disposition (correlation of electron density) function $z(x)$ in this case can be written as

$$z(x) = \delta(x) + \sum_{n=1}^{n=\infty} [H_n(x) + H_n(-x)] \tag{2a}$$

where H_n is the probability distribution of the nth neighbor, between simply the n-fold convolution of H_1 and $\delta(x)$ is the Dirac δ function. In deriving eq 2a, we supposed that there is no long-range, crystalline order in the system, and only the nearest-neighbor probability distribution need be specified. The disorder is therefore liquidlike, and only the average separation between the nth neighbors can be calculated:

$$\int_{-\infty}^{+\infty} xH_n(d_{Bragg} - x)\, dx = nd_{Bragg} \tag{2b}$$

Assuming the Gaussian form eq 1a, the Fourier transform of eq 2a can be easily obtained, yielding the intensity of the scattered radiation as a function of the wave vector ($I(Q)$). The intensity function in Q space displays peaks at multiples of $1/d_{Bragg}$ that grow progressively broader and finally merge with the background. A relation between the integral line width of the intensity function (ΔQ_n) at the nth diffraction peak in Q space defined as

$$\Delta Q_n = \int I(Q)\, dQ \tag{3a}$$

(over nth peak) and Δ_{Bragg} can be derived in the form[17]

$$\Delta Q_n = \frac{n^2\pi^2}{d_{Bragg}}(\Delta_{Bragg}/d_{Bragg})^2 \tag{3b}$$

The parameter Δ_{Bragg} characterizes the positional disorder of the Bragg planes (cf. eq 1a). Using now the hexagonal symmetry of the collapsed phase, we can derive a relation between the integral line width of the first peak in the intensity function in Q space and the positional disorder Δ_i in the interhelical spacing d_i

$$\Delta Q_1 = (2\pi^2/3^{1/2}d_i)(\Delta_i/d_i)^2 \tag{3c}$$

ΔQ_1 was determined by taking the first moment of the digitized diffraction pattern after subtracting the background scattering and plotting the difference versus Q. We obtain an effective Gaussian curve whose first-order integral line width ΔQ_1 can be measured directly, and Δ_i can be computed from eq 3c.

The measurements of osmotic pressure (Π) vs interhelical spacing were converted into the force per unit length ($f(d_i)$) vs spacing curves by observing that

$$f(d_i) = \Pi d_i/3^{1/2} \tag{4}$$

from the hexagonal symmetry of the DNA array.[1] Plotting log $f(d_i)$ vs interhelical spacing, d_i, shows that this transformation partly removes a slight curvature present in the plot of log Π vs

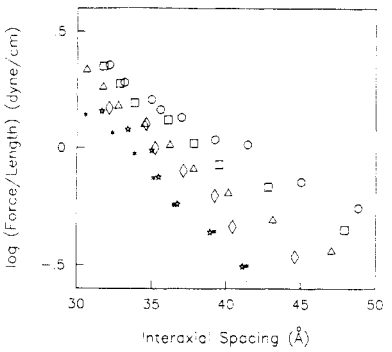

Figure 2. Force per unit length ($f(d_i) = \Pi d_i/3^{1/2}$) vs interaxial spacing d_i for DNA in 0.2–2.0 M NaCl solutions: ○, 0.2 M; □, 0.3 M; △, 0.4 M; ◇, 0.8 M; *, 1 M; ☆, 2 M. The error in the interhelical spacing determination is close to 1 Å. Actual physical contact between double helices is at d_i equal to the molecular diameter of ≅20 Å.

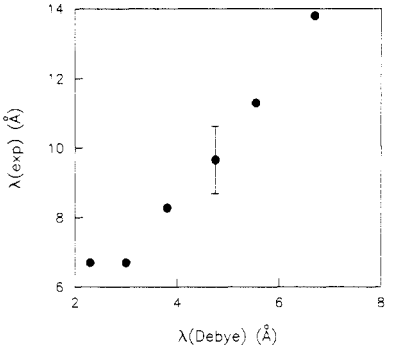

Figure 3. Apparent exponential decay constant λ_{exptl} vs theoretical electrostatic double-layer $\lambda_{Debye} \cong 3$ Å$/I^{1/2}$ for NaCl concentrations in the range I = 0.2–2.0 M (cf. Figure 2). Except at very high salt concentrations (≅1 M) where λ_{exptl} approaches a constant value equal to 6–7 Å, the observed decay rate is approximately twice that theoretically expected. The overall accuracy in the determination of the decay lengths is 10%. N.B. decay lengths are for exponentially decaying force per unit length $f(d_i) = \Pi d_i/3^{1/2}$ and are based on *all* the data given in Figure 2.

d_i. The decay constants reported below are therefore extracted after effecting this transformation and are some 10% different from the values obtained directly from the log Π vs d_i plot.

Results

Native Calf Thymus DNA in NaCl Solutions. 1. Force vs Distance Relations. Figure 2 shows the force per unit length ($f(d_i)$), as defined in Materials and Methods, acting on the DNA lattice vs interaxial distance d_i in the range 30–50 Å (corresponding to mean intersurface distances of 10–30 Å). Both the apparent rate of decay, obtained from the plot of force per unit length vs interhelical spacing for the reasons described above (cf. Materials and Methods), and the coefficient of the force per unit length are clearly sensitive to solution ionic strength. We have taken the exponential decay lengths λ_{exptl} from all these data points and plotted them in Figure 3 vs the Debye decay lengths λ_{Debye} obtained from the standard double-layer theory for the 0.2–2 M NaCl data shown in Figure 2. The standard error in λ_{exptl} is estimated at about 10%.

At NaCl concentrations between 0.1 and 0.8 M the relation is linear but with approximately twice the slope expected from double-layer theory alone. At large ionic strengths, 1 and 2 M NaCl, the observed decay length levels off to a constant 6–7 Å, close to twice the 3.4-Å decay seen for DNA at smaller separations (d_i < 30 Å) in 1 M NaCl, where hydration forces had been seen to dominate over electrostatic interactions.[1]

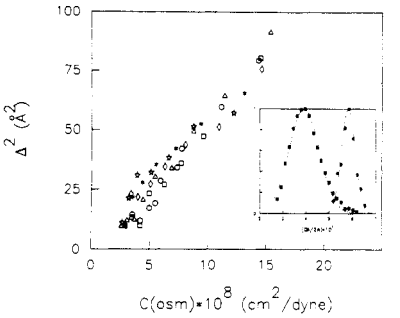

Figure 4. Lattice fluctuations measured as Δ_i^2, from X-ray scattering peak widths, vs lattice compressibility $C_{osm} = [d_i(\partial\Pi/\partial d_i)_T]^{-1}$. The data, same symbols as in Figure 2, now fall essentially onto one broad but common line whose slope suggests effectively independently moving segments some 45 Å in length. The inset shows the measured normalized and background scattering adjusted diffraction intensities as a function of the dimensionless wave vector ($Q\lambda/2\pi$) for the first and the last points of the 0.4 M NaDNA force curve (cf. Figure 2). The solid symbols represent measured points; the dotted curves show the least-squares Gaussian fit to the diffraction intensity.

2. Molecular Disorder. In order to examine the possibility that positional disorder in the interhelical spacings is a source of the differences in decay lengths between the predictions of the Poisson–Boltzmann theory and the results of the direct measurements, we have analyzed the progressive broadening of the X-ray diffraction pattern as a function of the mean interaxial separation d_i from d_i = 30 to 50 Å.

Is the mean square displacement $(\Delta_i)^2$ simply related to the measured system compressibility? We may think of the entire lattice as a collection of independently fluctuating units of length $\mathcal{L}$. We examine the volume fluctuation of these segments of mean volume $V = \mathcal{L}(3^{1/2}/2)d_i^2$. Since in our case V and T are independent variables, we will have according to the general theory of thermodynamic fluctuations[18]

$$\langle(\Delta V)^2\rangle = -kT(\partial V/\partial\Pi)_T \qquad (5)$$

with kT being the thermal energy. Expressing V in terms of d_i and the length of the independently fluctuating unit of a single polymer in the hexagonal assembly, we can derive an equation connecting $\Delta_i^2 = \langle(\Delta d_i)^2\rangle$ with the functional dependence of Π on d_i:

$$\Delta_i^2 = -\frac{kT}{3^{1/2}\mathcal{L}}\left(\frac{1}{d_i}\frac{\partial d_i}{\partial\Pi}\right)_T \qquad (6a)$$

A plot of Δ_i^2, deduced from the integral line widths of the diffraction pattern (eq 3c), vs osmotic compressibility defined here as

$$C_{osm} = (1/2)V^{-1}(\partial V/\partial\Pi)_T = d_i^{-1}(\partial d_i/\partial\Pi)_T \qquad (6b)$$

is shown in Figure 4. (C_{osm} is computed by recognizing the exponential dependence of force per unit length from the plot of $f(d_i)$ vs d_i, see Figure 2). The linearity of this plot and the collapse of the data of Figure 2 onto one band of points suggest that (a) pattern broadening can be used as a measure of the energetically important molecular disorder, which is the relevant parameter in helical repulsion, and (b) one may think of these fluctuations as occurring over characteristic lengths of $\mathcal{L} \simeq 45$ Å.

In the range of interhelical separations of approximately 30–50 Å, the root mean square fluctuation in spacing between the molecules changes from approximately 3 to 9 Å. This indicates that the separation between molecular surfaces at small osmotic pressures can vary by as much as 50%. It should be understood that this quantitative

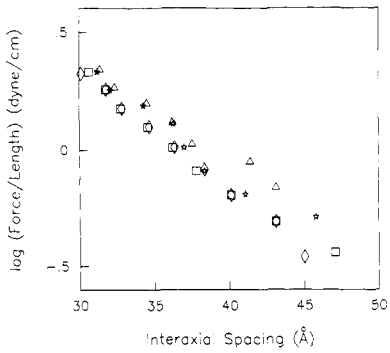

Figure 5. Weak effect of varying molecular stiffness on measured forces. $f(d_i)$ vs d_i for native CT-DNA (□), synthetic poly(dA-dT) (☆), synthetic poly(dG-dC) (◇), all of comparable length, and very short nucleosomal DNA (△).

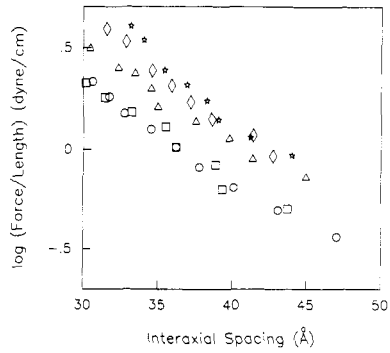

Figure 6. Forces measured in 0.4 M solutions of several different salts: ○, NaCl; □, LiCl; △, CsCl; ◇, $(CH_3)_4NCl$; ☆, $(C_2H_5)_4NCl$. Slopes are all quite similar (cf. Table I), but coefficients differ by a factor of 3.

estimate is an upper bound, corresponding to the assumption of essentially liquidlike behavior of the system, where all the broadening in the diffraction pattern is interpreted in terms of the positional disorder present in the DNA array. From the sharpness of diffraction peaks at high osmotic pressures, we infer that all other causes of broadening (e.g., finite domain size, X-ray system configuration) make only a small contribution to the overwhelming effect of positional disorder. To give some idea of the quality of the changes in line width, we have plotted (inset to Figure 4) the normalized diffraction intensity pattern for the first and the last points of the 0.4 M Na-DNA data set.

Figure 4 shows also that there is no sudden change in the molecular disorder present in the DNA array. The disorder builds up continuously. There is no indication of sudden, cooperative disordering that would discontinuously change the characteristics of the measured force curve. This qualitative result is independent of our approximate, semiquantitative treatment of the fluctuations in the spacing.

Polymers of Different Stiffness. To assess the generality of the observed changes in the force curve characteristics of collapsed DNA helices, we have compared the measured forces acting between native CT-DNA with those between synthetic copolymers that differ significantly in their "persistence length", a measure of elastic bending properties. For native DNA the value of the persistence length is approximately 600 Å. The corresponding value for poly(dA-dT) is between 250 and 300 Å and for poly(dG-dC) between 800 and 900 Å, respectively.[19] The measured forces for these three systems show no substantial variation either in magnitude or decay rate (Figure 5).

The high molecular weight CT-DNA fragments used here contain on the order of $\simeq 10^2$ persistence lengths. To see any effect of DNA length on interhelical forces, we prepared gels of nucleosomal DNA of slightly less than one persistence length ($\simeq$145 base pairs) in 0.4 M NaCl. The force decay length in this cage is slightly larger (Figure 5) than in the CT-DNA case, and the mechanical instability of the nucleosomal DNA gel at small osmotic pressures precludes a more quantitative statement.

Different Cationic Salts. To what extent does cationic species affect forces between collapsed double helices? The force measurement data for native CT-DNA in 0.4 M NaCl, LiCl, CsCl, $(CH_3)_4NCl$, and $(C_2H_5)_4NCl$ are displayed in Figure 6. It should be noted that at 0.4 M salt concentration the electrostatic forces still dominate the overall interaction between the helices at these distances, as can be clearly seen from inspection of Figure 2. There are, however, large differences in strength of repulsion of

Table I
Comparison between the Expected (Debye Decay Length) and the Measured Decay Lengths for Different Cationic Species[a]

molarity	ionic species	λ(expected), Å	λ(measured), Å
0.4	NaCl	4.7	9.6
	LiCl	4.7	9.2
	CsCl	4.7	9.6
	$(CH_3)_4NCl$	4.7	8.0
	$(C_2H_5)_4NCl$	4.7	7.8
2.0	NaCl	3.4	6.4
	LiCl	3.4	6.2
	$(CH_3)_4NCl$	3.4	7.3
	$(C_2H_5)_4NCl$	3.4	7.3

[a] At 0.4 M salt concentration the expected decay length is simply the Debye decay length at the specified salt concentration. At 2 M salt concentration the expected decay length is presumed equal to the hydration decay length observed at small interhelical spacings.[1] The overall accuracy in the determinations of the decay lengths is 10%.

as much as half an order of magnitude. The relatively small differences in apparent decay constant (Table I) are not systematic and are within the limits of experimental error.

At least to a first approximation it should be possible to use the theory of Manning[20] to estimate the magnitude of the forces determined by the amount of unneutralized phosphate charges on the DNA surface, which in turn depends on the degree of counterion condensation. According to the simplest version of this theory, there should be no variation in the surface charge or force magnitude with a univalent cation type. Our data suggest that the larger ions adsorb or condense very poorly to the surface, compared with Na^+, leaving more of the DNA phosphates unneutralized. This observation then is inconsistent with the widely used counterion condensation theory, unless it can be modified to include ion-specific binding.

Does ionic binding change with increasing osmotic pressure? We have no conclusive experimental data to rule out this possibility completely. We think, however, that the changes in ionic binding are inconsistent with the overall exponential dependence of osmotic pressure vs interhelical spacing as well as with the fact that the force curves remain essentially parallel for different ionic species in the whole range of measured osmotic pressures. If there are large changes in the ionic adsorption with interhelical spacing, there is no reason why the force curves for different ionic species should remain parallel at all spacings.

Forces in 2 M salt solutions (Figure 7) reveal yet additional features. Here, again, there is no significant difference in the magnitude of the forces or the decay lengths among the two bulkier cationic species (Table I).

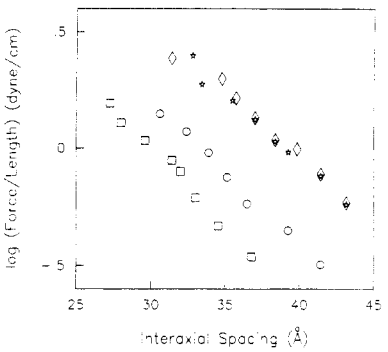

Figure 7. Forces measured in 2.0 M salt solutions: ○, NaCl; □, LiCl; ◇, $(CH_3)_4NCl$; ☆, $(C_2H_5)_4NCl$. Decay lengths here (cf. Table I), 6.2–7.3 Å, are twice the ≅3.4-Å decay length seen earlier[1] at higher pressures and smaller spacings (cf. Figure 8 below). There is almost 1 order of magnitude difference in the coefficient for DNA in solutions of different salts. We were unable to get a usable diffraction pattern from Cs-DNA at this salt concentration (cf. Materials and Methods).

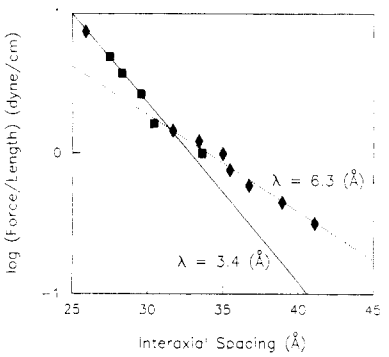

Figure 8. Force per unit length between parallel DNA double helices in 1 M NaCl showing both pure hydration force behavior (λ ≅ 3.4 Å) and fluctuation-enhanced hydration (λ ≅ 6.3 Å). Note transition at interaxial spacing of about 30 Å corresponding to an intersurface distance of about 10 Å. (■, data from ref 1; ♦, present work).

There is, however, a substantial difference in the magnitude of the forces (approximately 1 order of magnitude) measured in solutions of the two larger cationic species compared to those in NaCl or LiCl. Furthermore unlike the 0.4 M case, there is a large difference between Na-DNA and Li-DNA, similar to that seen in the hydration regime at shorter distances.[1] The measured decay lengths in 2 M salt solutions (Table I) are again approximately twice the hydration force decay lengths, observed at smaller interhelical spacings.

Discussion

The measurements of interhelical forces in polymer-condensed DNA arrays at interaxial separations greater than 30 Å reveal exponential forces whose decay rates are consistently slower than those expected from earlier theories.[28] In the regime where sensitivity to ionic strength suggests the action of electrostatic double-layer forces, the measured decay length is close to twice the Debye decay length (Figure 3). At larger salt concentrations, electrostatic forces appear effectively screened ($\lambda_{Debye} \leq 3$ Å). The measured decay length is close to twice the hydration decay rate known from measurements at small interhelical separations;[1] the force per unit length vs interhelical spacing curve clearly shows two different regimes of hydration repulsion whose decay rates differ by a factor of approximately 2 (Figure 8).

There is the question whether the results of the Poisson–Boltzmann theory,[28] used here to predict decay lengths of the expected forces, can be taken seriously in a DNA gel of hexagonal symmetry. Recent results of Jayaram et al.,[31] using a numerical solution of the nonlinear Poisson–Boltzmann equation for fixed charges at the PO_4^- positions on the B-DNA helix, support our assumption that the pure electrostatic double-layer (esdl) interaction is radially symmetric beyond 10 Å from the helix surface in 0.15 M univalent salt solution. At this salt concentration, and consequently at the higher salt concentrations we use here, this electrostatic double-layer potential is weak enough to justify the assumption that the interaction among a set of parallel elongated molecules is the pairwise sum of cylindrically symmetric interactions. We obtained the solutions of the Poisson–Boltzmann equation for radially symmetric cylinders in two different ways—either by considering a cell model of radially symmetric units or by the interaction of pairs of parallel rods. In both cases, solutions of the PB equation predict essentially exponential decay of forces with a λ_{Debye} decay constant over the range of ionic strengths we used in our measurements. It therefore seems appropriate to use the results of the simple Poisson–Boltzmann theory[28] to estimate the expected decay length.

It is worth noting that extended electrostatic repulsion was also observed in tobacco mosaic virus (TMV) gels and skinned muscle filament gels.[21,22] The decay rate extension in these systems is qualitatively consistent with our measurements. However, perhaps due to the large scatter in spacings intrinsic to those systems, one does not always see clearly the factor of 2 difference in decay lengths that is apparent in the DNA data. Still, for example, the average enhancement factor in the decay rate for repulsion between muscle filaments can be estimated at ≅1.9 with an average error of ≅15–20%.[22] Due to the larger spacings observed in this system, the PB theory should have worked even better than in the case of DNA gels. The modified Poisson–Boltzmann theory, proposed by Gruen and Marcelja[23] and invoked to explain the anomalously large decay lengths in muscle filament gels,[22] predicts variation in the effective force decay length with salt concentration, but that prediction amounts to a continuously varying ratio of $\lambda_{exp}/\lambda_{Debye}$ vs salt concentration rather than the factor of 2 seen here in the DNA data.

Extended repulsion at large intersurface separations has also been a salient and puzzling feature of electrostatic forces between charged phospholipid bilayers in multilayer arrays.[5] "Enhanced" electrostatic repulsion there has been ascribed to undulatory bending fluctuations of the interaction membrane surfaces.[9]

Theoretical Issues. While we expect that a proper theory of the extended decay of forces between DNA helices will be a nontrivial problem, we see three useful lines of reasoning that connect this behavior with lattice disorder.

1. Soft Collisions from Undulatory Fluctuations. Applied in the absence of strong van der Waals attraction, Evans and Parsegian's[9] theory of fluctuation-enhanced double-layer repulsion between bilayers predicts a logarithmic slope of exactly twice the classically expected value. However, the geometry of the collapsed DNA phase differs markedly from the planar geometry exploited in their calculations. In fact, that same theory predicts a logarithmic slope 4 times larger in a hexagonal array, a prediction due to inclusion of too high bending energies. Nevertheless, it appears to us that the underlying mechanisms responsible for the enhanced repulsion in the phospholipid and DNA cases are essentially similar.

2. Relation between Disorder and Compressibility. Configurational confinement is evident in the progressive broadening of X-ray diffraction peaks vs molecular separation. We have translated these peak widths into mean

square transverse displacements of the DNA helices. Figure 4 shows that the measure of the positional disorder in the hexagonal DNA array increases systematically with mean interhelical separation. The mean square transverse displacement changes from 10 to 90 Å^2, i.e., almost 10-fold, as the helices move apart.

The constant slope of the Δ_i^2 vs inverse compressibility (Figure 4) is what one would expect for independently fluctuating segments of a double helix each approximately 45 Å long. This length, from the slope of the straight line, is similar in a way to what one sees in the random walk theory of polymers in Θ solvents where one plots the radius of gyration squared vs the molecular length L to obtain the persistence length l_p, $R_g^2 = {}^1/_3 L l_p$.

To estimate the part of the free energy of the assembly that corresponds to the suppression of fluctuations, we have integrated our pressure curve obtained at 2 M salt concentrations from $d_i = 42$ to $d_i = 30$ Å. This integration gives a value of ≅0.1 kcal/mol for base pairs that is close to the value obtained by taking the difference of the terms $kT \ln \Delta_i^2$ at the two limiting values of the interhelical spacing if the independent fragment length is taken ≃45 Å. This correspondence gives additional strength to the argument that the interaction in this range of spacings is dominated by configurational entropy.

The effective intersurface separations to which the DNA helices can approach each other by fluctuations are significant compared with the mean spacings between the surfaces. The soft collisions that restrain molecular fluctuations actually occur with energies much greater than those expected from mean spacings and should therefore contribute significantly to the observed enhanced repulsion.

3. DNA Random Walk in a Tube of Its Neighbors. In a theory developed to understand the movement of flexible polymers through gels, Odijk[24,25] has shown how a natural step length, $\mathcal{L}$, such that $\mathcal{L}^3 \simeq l_p D^2$, characterizes the configurational statistics of a polymer of persistence length l_p confined to a tube of diameter D. In fact, the configurational part of the free energy of the confined polymer turns out to be inversely proportional to $\mathcal{L}$. Typically $\mathcal{L} \ll l_p$ if $D \ll l_p$, and $\mathcal{L}$ will be a weak function of l_p. The action of forces from neighboring molecules in the hexagonal lattice of collapsed DNA creates restoring forces different in action from the hard walls of Odijk's tube; we suspect that the addition of a soft force field to a random walk model with a step length $\mathcal{L}$ would probably capture the essential features of the behavior we observe.[30]

Ion Binding and Repulsive Forces. While the decay length of the force curves is a function of the ionic strength, there appears to be no significant variation with cationic type. This is not the case for the absolute magnitude of the force. Its variation (Figures 6 and 7) with cationic type is much more pronounced than changes due to the ionic strength (Figure 2). One expects from the simplest PB theory that the magnitude of an electrostatic force depends on the magnitude of the large negative charge of phosphates on the DNA surface. This charge is, as suggested by Manning[20] on the basis of electrostatic interactions, almost completely balanced by adsorbed cations irrespective of cation type. But our measurements of forces in different salts show significant qualitative difference in magnitude with insignificant differences in decay length. At 0.4 M univalent salt concentration the amount of charge compensation at the surface is clearly a function of cationic size (Figure 6). Li^+ and Na^+ allow only a small residual charge while the bulkier hydrophobic ions $N(CH_3)_4^+$ and $N(CH_2CH_3)_4^+$ are not able to compensate the phosphate charge to the same extent. The Manning theory is not designed to explain these differences in the magnitude of active polyelectrolyte charge in different univalent salts. The dependence of the magnitude of the force at small ionic strengths on the type of cation compares well with the data on fractional charge per phosphate obtained from the measurements of mobility of different DNA salts. The fractional charge per phosphate was found to be 0.33, 0.36, and 0.43 for Li^+, Na^+, and tetramethylammonium ion, respectively.[26] The relative progression in the amount of fractional charge for different cationic species is qualitatively followed by the relative progression in the magnitude of the forces (Figure 6).

Hydration Forces and Fluctuation-Enhanced Hydration Forces. In high salt concentration solutions (>1 M), with Debye lengths less than ≅ 3 Å (the decay length associated with the hydration force), electrostatic double-layer forces are effectively screened out. There is then an interplay between entropic confinement and hydration forces. At larger separations (15–30 Å between surfaces) one observes fluctuation-enhanced hydration forces with an empirical, ionic strength independent decay constant of some 6–7 Å. As the molecules approach contact (intersurface separation ≅ 10 Å) fluctuations are lost; the force reverts to the ≅3-Å decay characteristic of the underlying hydration force between double helices.[1] This observation in turn rules out the possible interpretation of the hydration force as a modified short-range electrostatic interaction. Since in the fluctuation-enhanced form it clearly persists to large separations.

Because the extent of water polarization around hydrophobic cations is relatively small[29] and because our force measurements in the electrostatic regime (Figure 6) suggest poor adsorption (high fractional charge per phosphate) to the DNA surface, it might be that the fluctuation-enhanced hydration force seen at high tetramethyl and tetraethyl ammonium concentrations reflects mainly the great strength of water perturbation by the DNA phosphate and sugar groups. In contrast, Li^+ is a strongly hydrated, strongly adsorbing species. The data of Figure 7 suggest a relatively weaker net polarization of water at the Li-DNA surface, evidence for a cancellation of the opposite polarizing tendencies of fixed phosphates and adsorbed cations. Differences in hydration forces of Li-DNA and Na-DNA might therefore be rationalized in terms of the cations' differing hydration properties, while their similar electrostatic double-layer properties suggest similar degrees of adsorption.

Forces in DNA Assembly. The direct measurements of interaction between DNA helices reported here and before,[1] covering the range of interhelical spacings from approximately 25–50 Å, clearly give a good idea of what is happening during the assembly of DNA helices as they collapse from the bulk solution. The collapse free energy has essentially only two major contributions: first from the suppression of the fluctuations in the shape of the molecules upon mutual approach and second from the subsequent dehydration of their surfaces as they approach even closer.

Invoking the condensation theory of Post and Zimm,[27] we find that the free energy of collapse estimated from the integration of the force curves is consistent with their calculated values if the interaction parameter χ is just slightly above the "condensation" value. It is, however, difficult to compare predictions of the Post and Zimm model, which describes the collapse of a single polymer molecule where the interaction between the segments is essentially just the excluded volume with the free energy

that we get from our osmotic pressure data, which in fact describes the detailed nature of the "excluded volume".

Contrary to the view that direct electrostatic double-layer interactions make an important contribution in the assembly of DNA helices, the factor-of-2 difference in the decay constants (Figure 3) suggests that they are in fact negligible. They do show up in an important way only indirectly through the entropic work needed to suppress the positional disorder of the chains on their close approach. In fact, given the importance of fluctuations in systems as diverse as bilayers and condensed DNA double helices, one is led to suggest that electrostatic double-layer forces are unlikely ever to appear between flexible molecules without the qualitative enhancement imposed by molecular disorder. Conversely one is now aware of a systematic relation between the disorder and the forces which act to suppress it.

In this connection it is worth noting that the exponential decay of the forces observed here does not have the power law form expected for the steric repulsion between hard flexible rods.[25,32] There seems to be no experimental justification in our data for the assumption, virtually universal in theories of liquid-crystal packing, that charged particles in salt solution can be portrayed as hard particles with an effective radius adjusted according to ionic strength.

Acknowledgment. We are pleased to thank Charles Bean, Victor Bloomfield, Evan Evans, Sol Gruner, Gerald Manning, and Bruno Zimm for careful reading of a preliminary draft and for useful suggestions improving this text. We are grateful to Benes Trus of the Division of Computer Research and Technology, NIH, for allowing us to use their optical densitometer with related software.

References and Notes

(1) Rau, D. C.; Lee, B. K.; Parsegian, V. A. *Proc. Natl. Acad. Sci. U.S.A.* **1984**, *81*, 2621.
(2) Leneveu, D.; Rand, R. P.; Parsegian, V. A. *Nature (London)* **1976**, *259*, 601.
(3) Parsegian, V. A.; Fuller, N. L.; Rand, R. P. *Proc. Natl. Acad. Sci. U.S.A.* **1979**, *76*, 2750.
(4) Rand, R. P. *Annu. Rev. Biophys. Bioeng.* **1981**, *10*, 277.
(5) Lis, L. J.; Lis, W. T.; Parsegian, V. A.; Rand, R. P. *Biochemistry* **1981**, *20*, 1771.
(6) Loosley-Millman, M.; Rand, R. P.; Parsegian, V. A. *Biophys. J.* **1982**, *40*, 221.
(7) Pashley, R. M. *J. Colloid Interface Sci.* **1981**, *83*, 531.
(8) Marra, J.; Israelachvili, J. N. *Biochemistry* **1985**, *24*, 4608.
(9) Evans, E. A.; Parsegian, V. A. *Proc. Natl. Acad. Sci. U.S.A.* **1986**, *83*, 7132.
(10) Helfrich, W. *Z. Naturforsch.* **1978**, *33A*, 305.
(11) Parsegian, V. A.; Rand, R. P.; Fuller, N. L.; Rau, D. C. *Methods of Enzymology*; Packer, L., Ed.; 1986; p 127.
(12) Maniatis, T.; Venable, J. W., Jr.; Lerman, L. S. *J. Mol. Biol.* **1974**, *74*, 37.
(13) Shindo, H.; McGhee, J. D.; Cohen, J. S. *Biopolymers* **1980**, *19*, 523.
(14) Michel, B. E.; Kaufmann, R. M. *Plant Physiol.* **1973**, *51*, 914.
(15) Michel, B. E. *Plant Physiol.* **1983**, *72*, 66.
(16) Robinson, C. *Tetrahedron* **1961**, *13*, 219.
(17) Guinier, J. *X-ray Diffraction in Crystals, Imperfect Crystals and Amorphous Bodies*; W. H. Freeman: San Francisco, 1963.
(18) Landau, L. D.; Lifshitz, E. M. *Statistical Physics*; Pergamon Press: London, 1958.
(19) Hogan, M. E.; Austin, R. M. *Nature (London)* **1987**, *329*, 263.
(20) Manning, G. S. *Q. Rev. Biophys.* **1978**, *11*, 327.
(21) Millman, B. M.; Nickel, B. G. *Biophys. J.* **1980**, *32*, 49.
(22) Millman, B. M. *Electrical Double Layers in Biology*; Blank, M., Ed.; Plenum Press: New York, 1986; p 301.
(23) Gruen, D. W. R.; Marčelja, S. *J. Chem. Soc., Faraday Trans.* **1983**, *79*, 225.
(24) Odijk, T. *Macromolecules* **1983**, *16*, 1340.
(25) Odijk, T. *Macromolecules* **1986**, *19*, 2313.
(26) Bloomfield, V. A.; Crothers, D. M.; Tinoco, I., Jr. *Physical Chemistry of Nucleic Acids*; Harper & Row: New York, 1974.
(27) Post, C. B.; Zimm, H. B. *Biopolymers* **1979**, *18*, 1478.
(28) Parsegian, V. A. *Annu. Rev. Biophys. Bioeng.* **1973**, *2*, 222.
(29) Conway, B. E. *"Ionic Hydration in Chemistry and Biophysics". Studies in Physical and Theoretical Chemistry*; Elsevier: New York, 1981; Vol. 12.
(30) Podgornik, R.; Parsegian, V. A., manuscript in preparation.
(31) Jayaram, B.; Sharp, K. A.; Honig, B. *Biopolymers*, in press.
(32) Helfrich, W.; Harbich, W. *Chem. Scr.* **1985**, *25*, 32.

Surface-Interacting Polymers: An Integral Equation and Fractional Calculus Approach

Jack F. Douglas

National Bureau of Standards, Gaithersburg, Maryland 20899. *Received June 22, 1988; Revised Manuscript Received September 21, 1988*

ABSTRACT: A method due to Feynman and Kac is used to convert the path integral formulation of surface (variable surface dimension) interacting polymers into an equivalent integral equation approach. The integral equation for the surface-interacting chain partition function is determined to be the Volterra analogue of the Fredholm integral equation describing the friction coefficient in the preaveraged Kirkwood–Riseman theory. This approach to surface interacting polymers thus clarifies the close interconnection between the surface interaction and Kirkwood–Riseman theories noted in previous renormalization group calculations. An exact solution of the surface-interacting chain partition function is obtained by using the Riemann–Liouville fractional calculus. Finally, the integral equation and fractional calculus methods are combined to explain some of the most conspicuous features of the renormalization group theory—the mathematical significance of the "crossover exponent", "infrared fixed point", nontrivial "critical exponents", and the pole structure found in the interaction perturbation theory. The integral equation–fractional calculus formalism is also used to examine a point of "critical instability" defining the adsorption threshold and to examine the failure of the renormalization group and eigenfunction expansion methods to describe scaling functions for values of the interaction near the instability point. The critical instability is readily understood on the basis of the Fredholm alternative.

1. Introduction

Recent renormalization group (RG) treatments of surface-interacting[1,2] and hydrodynamically interacting polymers[3,4] indicate a remarkably similar common analytic structure. In many cases the results from one theory can be applied to the other by simply changing the interaction labels.[2] This correspondence holds even when excluded volume is additionally incorporated into the surface and hydrodynamic interaction theories.[2]

The origin of this unity in the underlying mathematical structure of these models of interacting polymers is not immediately evident but is well worth investigating. It is